Plasma Sintering of New Carbide Electrodes†

Masao USHIO*, Kenji IKEUCHI, Manabu TANAKA*** and Tsuyoshi HAYASHI******

Abstract

In order to develop electrodes that can withstand use in arc plasmas involving reactive gases such as Cl_2 and O_2, TaC and HfC have been sintered by plasma. The sintered carbides exhibited excellent performances as electrodes for arc plasmas involving the reactive gases. The sintering plasma was generated in an Ar atmosphere from 40 kPa to 53 kPa by an rf power operating at 13.56 MHz. High-density TaC with a relative density of about 93% was produced with a sintering time of 3.6 ks when the rf output power was 5 kW and the atmospheric pressure was 53 kPa. No significant densification of HfC, however, was observed after the sintering under the same conditions. Addition of 30% Hf powder accelerated greatly the densification of the HfC powder, resulting in the attainment of relative density of about 89% under the same sintering conditions. The sintered TaC and HfC with 30% Hf were applied for the cathodes of atmospheric arcs involving Cl_2 and O_2, respectively. Both of these carbide electrodes showed excellent arc stability and durability compared with the conventional electrodes.

KEY WORDS: (Plasma Sintering) (Rf Plasma) (TaC) (HfC) (Plasma Electrode) (Waste-Material Disposing) (Active Gases)

1. Introduction

The carbides TaC and HfC have lower work functions and higher melting points than tungsten, a major electrode material for arc discharge (**Fig. 1**). It has also been suggested that these carbides have excellent durability in plasma atmospheres involving reactive gases such as Cl_2 and O_2[1,2,3]. In recent years, attempts have been made to apply the arc plasma for the disposal of waste materials in which the atmosphere contains reactive gases[4]. For this, the development of new electrode materials that can endure the plasma atmosphere involving the reactive gases is desirable.

In this respect, TaC and HfC can be regarded as promising candidate materials satisfying requirements for the electrode of plasmas for disposal of waste materials. However, having very high melting points, these carbides are difficult to melt, cast or sinter. To our knowledge, there has been no report of the production of bulk specimens of these carbides having dimensions and shapes suitable for use as electrodes.

The present study has been undertaken to sinter these carbides by taking advantage of the Ar rf plasma, which can yield higher temperatures than other conventional heat sources for sintering. The performance of the sintered carbides as the electrode has also been investigated in plasmas involving Cl_2 and O_2.

2. Experimental Details

The compositions of the TaC and HfC powders used are shown in **Table 1**. The particle sizes of TaC and HfC were about 1 μm. The powder was subjected to preliminary sintering at temperatures between 1500 and 1800 K to prepare rectangular specimens 3x3x30 mm prior to the plasma sintering. Specimens of three different compositions were prepared: (1) specimens consisting of the TaC powder alone (abbreviated to TaC specimen), (2) specimens consisting of the HfC powder alone (abbreviated to HfC specimen), and (3) specimens consisting of the HfC powder (70%) and metal Hf powder (30%) (abbreviated to 30%Hf+HfC specimen). Sintering was performed in Ar plasmas driven by radiofrequency (rf). **Figure 2** is a schematic illustration of the apparatus for the rf plasma sintering. This apparatus was composed of an rf generator (maximum output = 5 kW,

† Received on May 24, 1996
* Professor
** Associate Professor
*** Research Associate
**** Graduate Student (Presently at Toyota Motor Car Co. Ltd.)
Transactions of JWRI is published by Joining and Welding Research Institute, Osaka University, Ibaraki, Osaka 567, Japan

Table 1 Chemical compositions and particle sizes of the HfC and TaC powders.

Powder	Particle size	Chemical composition (%)		
		Total.C	Free.C	O
HfC	1.28 μm	6.33	0.39	0.13
TaC	1.00 μm	6.3	0.1	0.1max

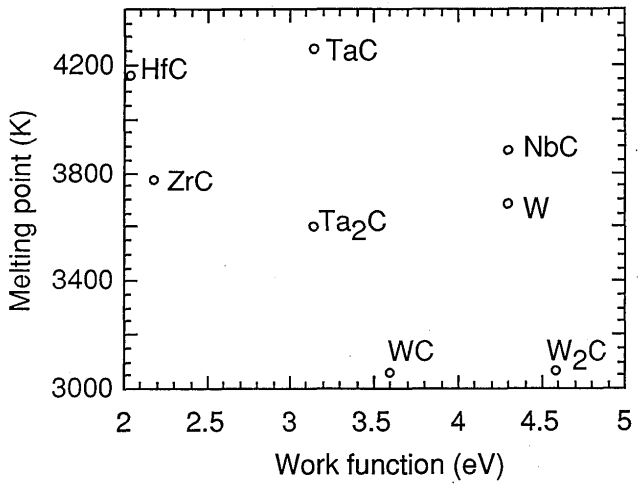

Fig. 1 Work function vs. melting point of candidate materials for the electrode.

frequency = 13.56 MHz), a water-cooled process chamber (18 mm in inner diameter), a supply of working gas (Ar), a vacuum pump, and an actuator to move the specimen. The sintering was carried out at pressures between 40 and 53 kPa and Ar flow rates between 1 and 4 l/min.

3. Results and Discussion

3.1 Temperature of specimen during sintering

In order to estimate the temperature of the specimen held in the rf Ar plasma, refractory metals - hafnium, niobium, molybdenum, tantalum and tungsten, having almost same dimensions as the sintering specimen were held in the plasma, and melting phenomena of these metals were observed. The results are shown in **Table 2**. The hafnium, niobium and molybdenum specimens were melted at a holding time of about 15 s, while the tantalum specimen was melted only at the tip after a long holding time. The tungsten specimen was not melted at all. From these results, the temperature of the specimens held in the rf Ar plasma was estimated to be about 3300 K.

3.2 Plasma sintering of TaC

When the TaC specimen was sintered in the plasma, a surface layer having a microstructure different from the

Table 2 Melting of refractory metals by exposure to the Ar plasma driven by radiofrequency of 5 kW.

Material	Melting point	Melt
Tungsten	3683 K	No
Tantalum	3269 K	Yes (after long exposure)
Molybdenum	2893 K	Yes
Niobium	2741 K	Yes
Hafnium	2498 K	Yes

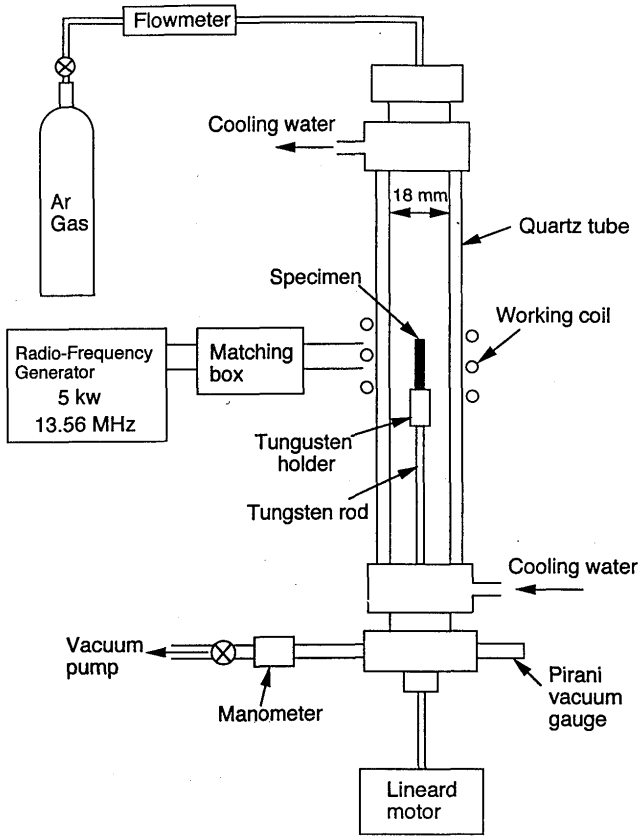

Fig. 2 Schematic diagram of the apparatus for the rf-plasma sintering.

bulk region was formed as shown in **Figs.3 (a)** and **3(b)**. In **Figs.4** and **5**, X-ray diffraction patterns from the surface and bulk regions of a sintered TaC specimen are shown. Diffraction lines indicating the presence of metal Ta and Ta_2C were observed from the surface, and only diffraction lines from TaC were detected from the bulk region of the specimen. These results suggest that the plasma-sintered TaC specimen consisted mostly of TaC except for the decarburized surface layer of about 100 μm thickness.

The evolution of the bulk microstructure with

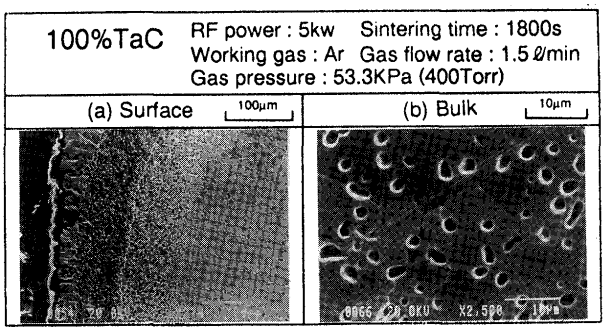

Fig. 3 SEM micrographs of a plasma-sintered TaC specimen: (a) surface region and (b) bulk region.

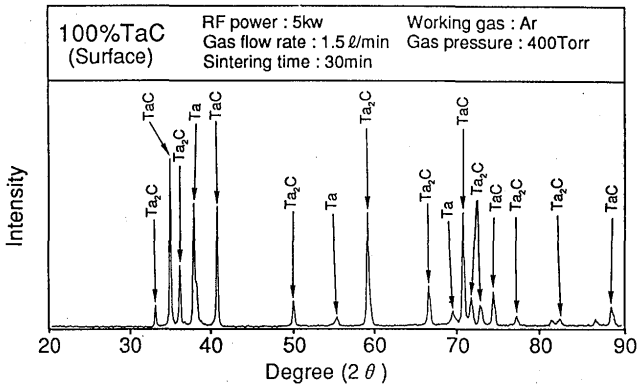

Fig. 4 X-ray diffraction pattern from the surface of a plasma-sintered TaC specimen.

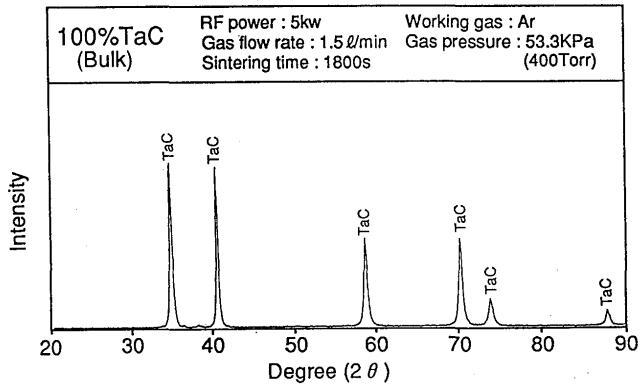

Fig. 5 X-ray diffraction pattern from the bulk region of a plasma-sintered TaC specimen.

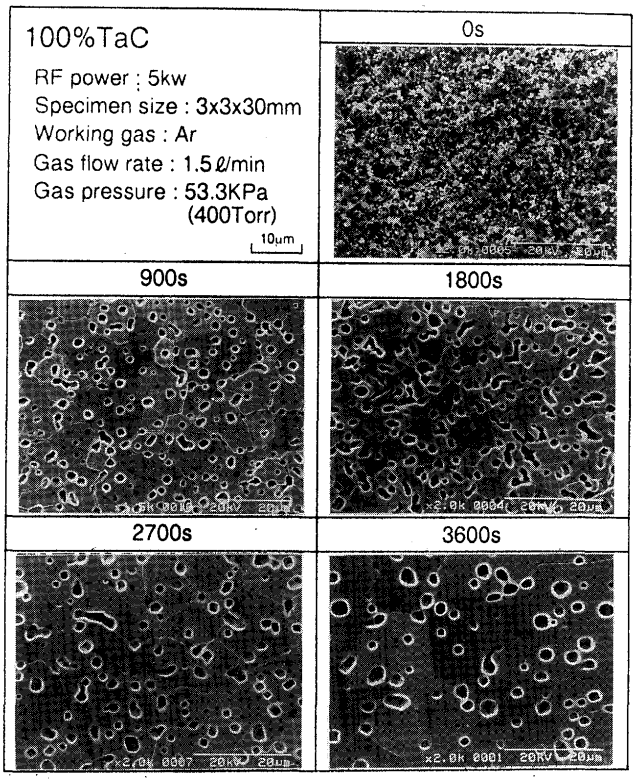

Fig. 6 Effect of sintering time on the bulk microstructure of the plasma-sintered TaC specimen.

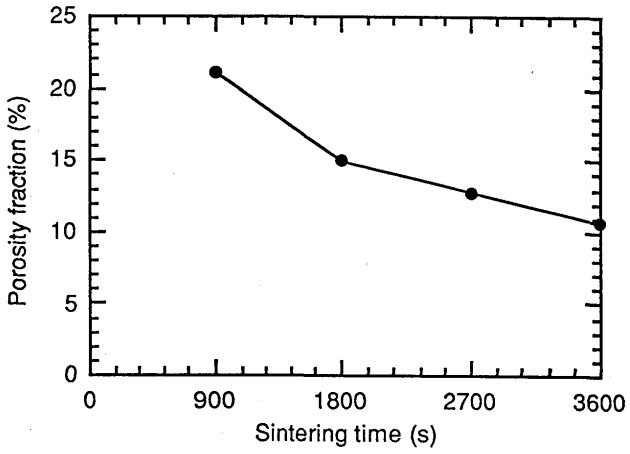

Fig. 7 Relation between the volume fraction of porosities and sintering time in the plasma sintering of the TaC specimen.

sintering time is shown in **Fig. 6**. As the sintering time was increased, the porosity coalesced and its volume fraction decreased. The grain size increased with sintering time. In **Fig. 7**, the volume fraction of porosities is plotted against the sintering time. The porosity fraction decreased to 11% at a sintering time of 3.6 ks.

The TaC specimens sintered for 3.6 ks were formed into electrodes 2.4 mm in diameter and 25 mm in length by grinding, and were applied to an Ar arc plasma involving 10% Cl_2, to evaluate the performance of the sintered TaC. Electrodes of TaC working in the plasmas at arc currents of 50 A to 200 A are shown in **Fig. 8**. Conventional electrodes of W-ThO_2 were also applied in the arc plasma under the same conditions for comparison. When the TaC electrode was used, the arc discharge was stable, although the tip of the electrode was melted slightly. When the W-ThO_2 electrode was used, on the other hand, deposits were formed on the side surface of

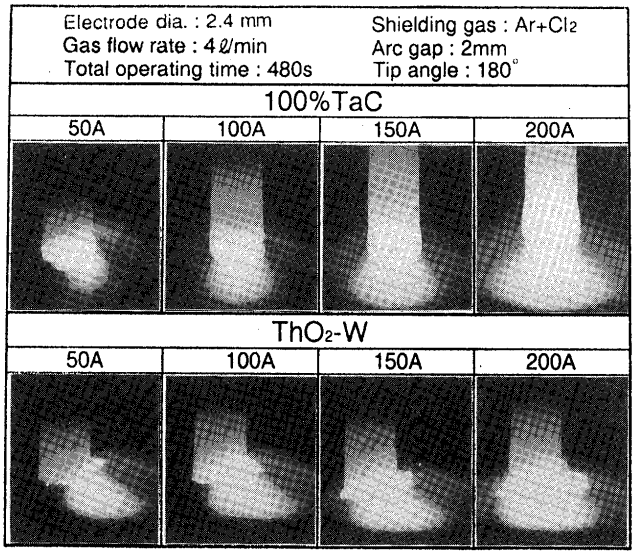

Fig. 8 Photographs of arc plasmas and electrodes of plasma-sintered TaC and W-ThO_2 during arc discharge at currents from 50 to 200 A in Ar + 10% Cl_2.

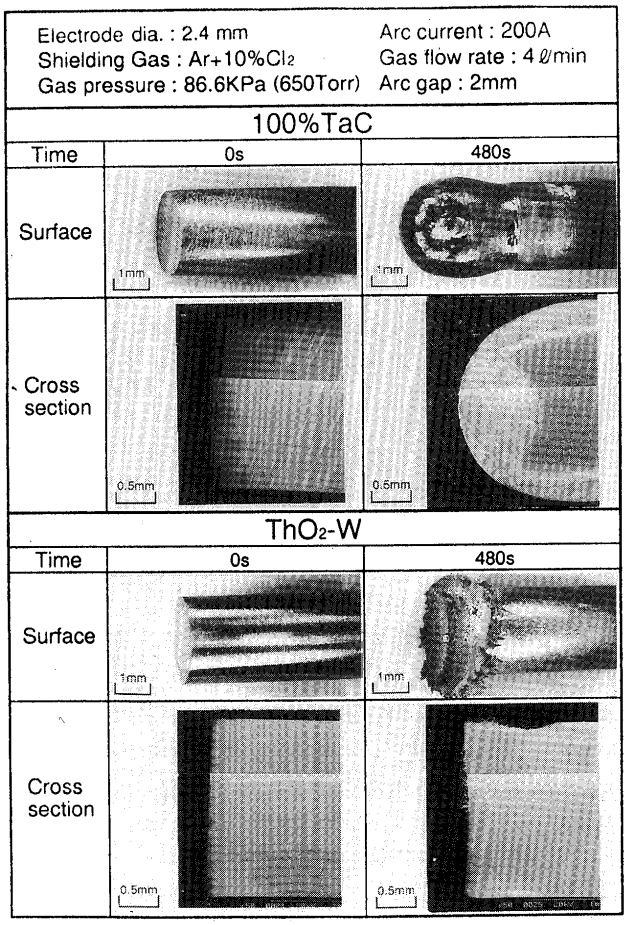

Fig. 9 Appearance and SEM micrographs of TaC and W-ThO_2 electrodes after arc discharge for 480 s in Ar + 10% Cl_2.

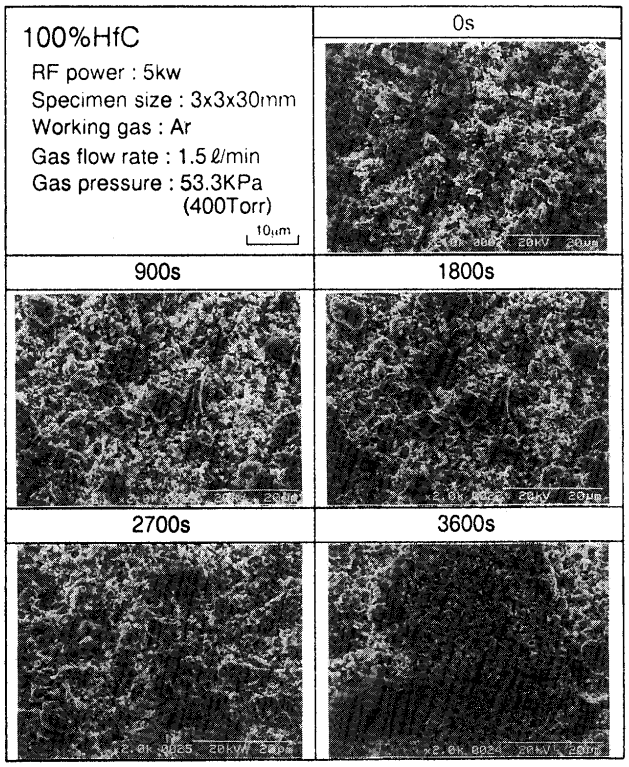

Fig. 10 Effect of sintering time on the bulk microstructure of the plasma-sintered HfC specimen.

the electrode close to its end, and the arc became quite unstable. The appearances and microstructures of the TaC and W-ThO_2 electrodes after the arc discharge are shown in **Fig. 9**. Quite large amounts of deposit were visible at the tip of the W-ThO_2 electrode, and the consumption of the electrode was also quite severe. The TaC electrode was less consumed than the W-ThO_2 electrode, although slight melting was observed at the tip.

From these results, it can be concluded that the TaC electrode has excellent durability in the plasma involving Cl_2, even at high currents, as compared with the W-ThO_2 electrode.

3.3 Plasma sintering of HfC

When the HfC specimen was sintered in the plasma, no significant densification was observed as shown in **Fig. 10**, although the plasma parameters employed were the same as those of the TaC specimen. At the surface of the specimen a layer, about 50 μm thick, was observed as shown in **Fig. 11**. As shown in **Fig. 12**, the X-ray diffraction pattern from the surface indicated the formation of HfO_2 at the surface, suggesting that oxidization had occurred during the sintering.

When the 30%Hf+HfC specimen was sintered in the plasma under the same conditions an oxidized layer, similar to that observed in the HfC specimen, was also

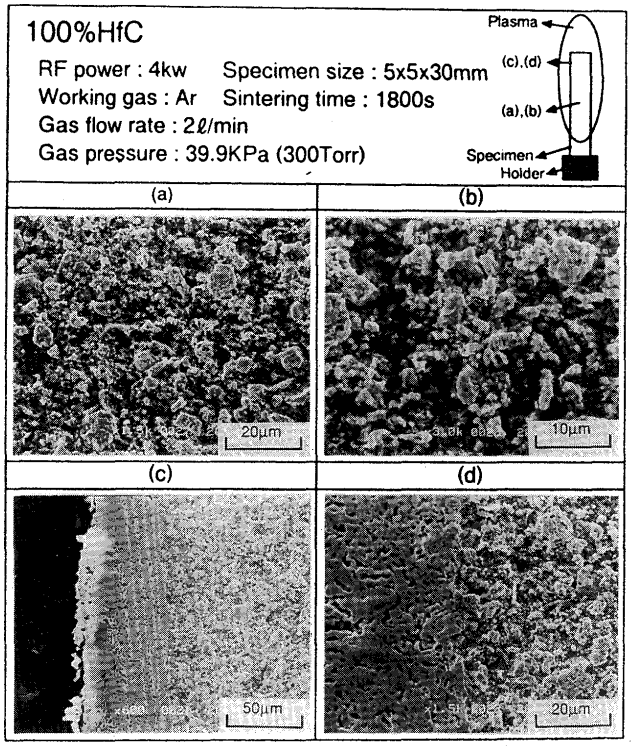

Fig. 11 SEM micrographs of a plasma-sintered HfC specimen. Observation areas (a), (b), (c) and (d) are indicated in the inset.

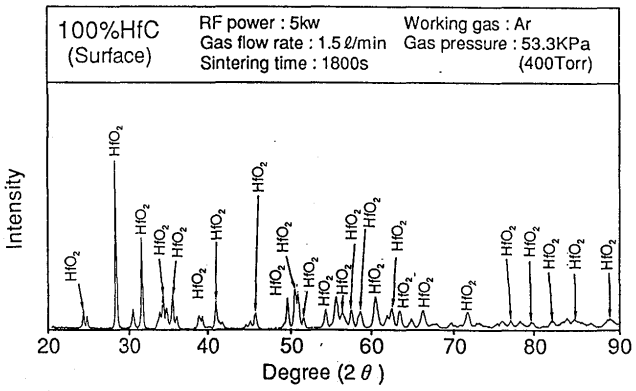

Fig. 12 X-ray diffraction pattern from the surface of a plasma-sintered HfC specimen.

formed at the surface (**Fig. 13**), but significant densification occurred in the bulk region (**Fig. 14**). As can be seen in Fig. 14, the volume fraction of porosities decreased, and the grain size increased as the sintering time was increased. In **Fig. 15**, the volume fraction of the porosity is plotted against the sintering time. The porosity fraction decreased to 14% at a sintering time of 3.6 ks. In **Fig. 16**, the X-ray diffraction pattern from the bulk region of a sintered 30%Hf+HfC specimen is shown. Only diffraction lines from HfC were detected from the bulk region of the specimen, suggesting that the

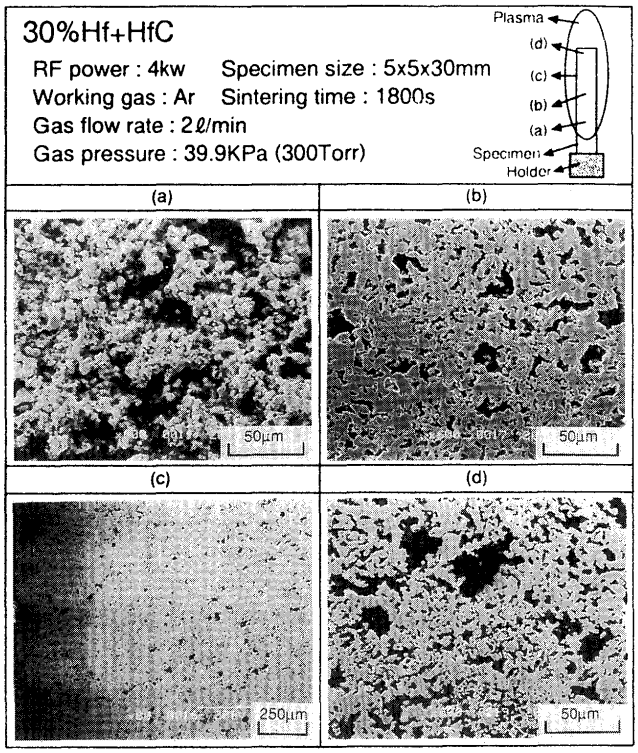

Fig. 13 SEM micrographs of a plasma-sintered 30%Hf+HfC specimen. Observation areas (a), (b), (c) and (d) are indicated in the inset.

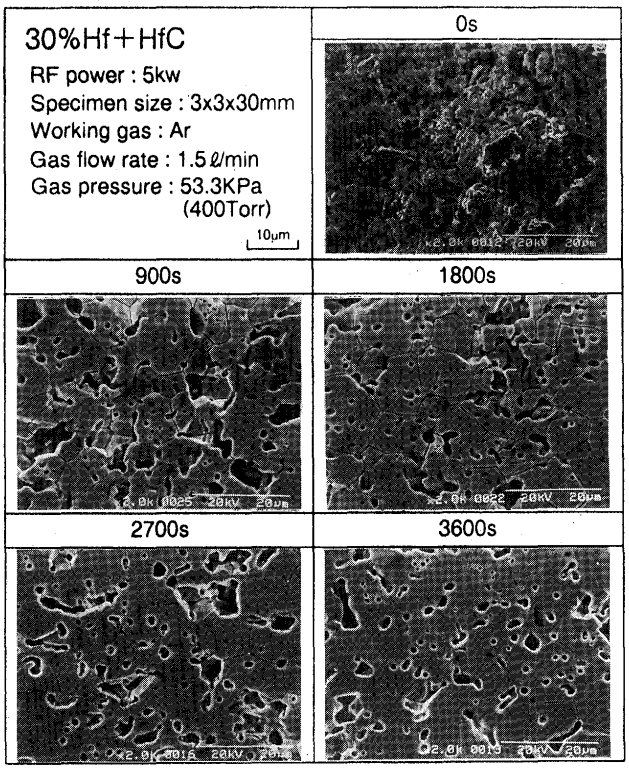

Fig. 14 Effect of sintering time on the bulk microstructure of the plasma-sintered 30%Hf+HfC specimen.

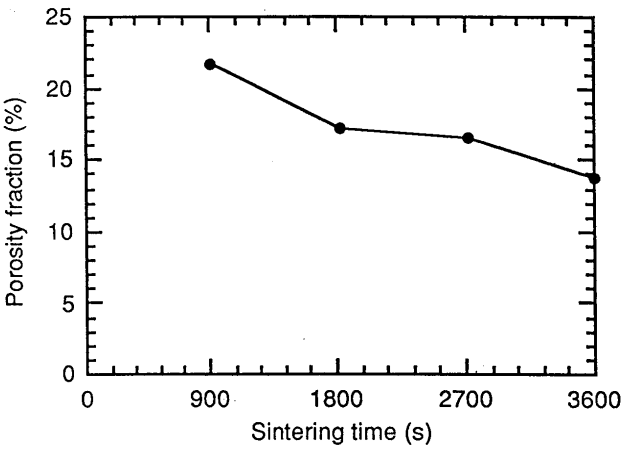

Fig. 15 Relation between the volume fraction of porosities and sintering time in the plasma sintering of the 30%Hf+HfC specimen.

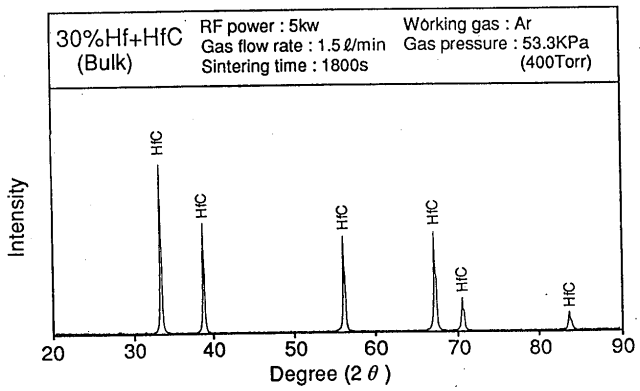

Fig. 16 X-ray diffraction pattern from the bulk region of a plasma-sintered 30%Hf+HfC specimen.

specimen consisted mostly of HfC. This is probably due to the wide solid solution range of HfC in Hf-C binary system and the presence of free carbon in the HfC powder (see Table 1).

The specimen of 30%Hf+HfC sintered by the plasma for 3.6 ks was also formed into an electrode having same dimensions as those of the TaC specimen, and was applied as an electrode for an air arc plasma. Electrodes of 30%Hf+HfC working in air plasmas are shown in **Fig. 17**. Conventional electrodes of Hf were also applied to the air plasma under the same conditions for comparison. When the Hf electrode was used, the arc discharge was quite unstable because of the irregular movement of the cathode spot. When the 30%Hf+HfC electrode was used, the arc discharge was stable. The appearances and microstructures of the 30%Hf+HfC and Hf electrodes applied to the arc discharge are shown in **Fig. 18**. A large melted area involving cracks was observed at the tip of the Hf electrode, while the melted

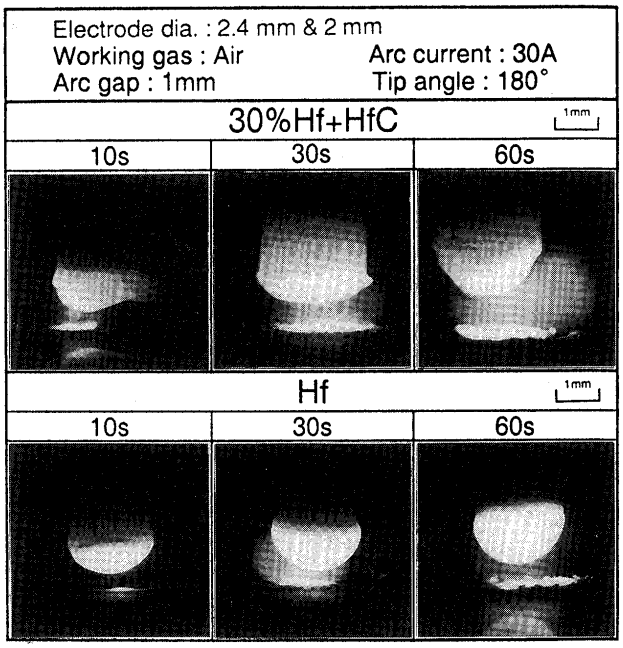

Fig. 17 Photographs of arc plasmas and electrodes of plasma-sintered 30%Hf+HfC and Hf during arc discharge at a current of 30 A in air.

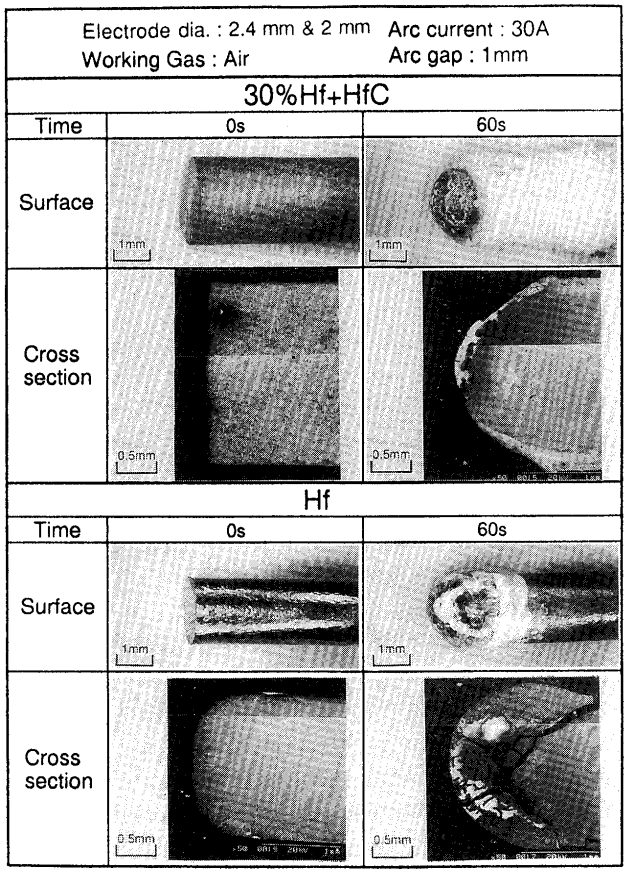

Fig. 18 Appearance and SEM micrographs of 30%Hf+HfC and Hf electrodes after arc discharge for 60 s in air.

area of the 30%Hf+HfC electrode was narrower and cracks were not observed.

From these results, it can be concluded that the 30%Hf+HfC electrode has better durability in the plasmas involving O_2 than the Hf electrode.

4. Conclusion

Ar plasmas generated by radiofrequency of 13.56 MHz were applied for the sintering of carbides TaC and HfC having high melting points, low work functions and excellent durability to atmospheres involving reactive gases. High density TaC with a porosity fraction of about 11% was produced by the plasma sintering. However, no significant densification was observed for the HfC specimen even after plasma sintering under the same conditions. Addition of 30% Hf powder greatly accelerated the densification of the HfC specimen, resulting in the attainment of a porosity fraction of about 14%. The sintered TaC and 30%Hf+HfC specimens were applied as the cathodes of atmospheric arc plasmas containing Cl_2 and O_2, respectively. Both of these carbide electrodes exhibited excellent arc stability and durability compared with the conventional electrodes.

References

1) R.B. Kotelinikov, S.N. Bashilikov, Z.G. Galiakbalov, and A.I. Kashtanov: Reference Book "Ultra-Refractory Elements and Componds", Metallurgy Publishing, Moscow, (1969).
2) K. Shanker, P.G. Tsantrizos, L.T. Mavropoulos and R.A.L. Drew : "Electrode properties of TaC-metal matrix composites", *Development and Applications of Ceramics and New Metal Alloys*, 177-184 (1993).
3) E.T. Turkdogan : "The Elements", *Clarendon Press*, (1989).
4) Plasma Technology for a Better Environment, UIE, (1992).